Published OnlineFirst July 20, 2010; DOI: 10.1158/0008-5472.CAN-10-0015
Published OnlineFirst on July 20, 2010 as 10.1158/0008-5472.CAN-10-0015

Cancer Research

A Chemosensitization Screen Identifies TP53RK, a Kinase that Restrains Apoptosis after Mitotic Stress

David Peterson[1], James Lee[2], Xingye C. Lei[3], William F. Forrest[3], David P. Davis[2], Peter K. Jackson[1], and Lisa D. Belmont[1]

Abstract

Taxanes are very effective at causing mitotic arrest; however, there is variability among cancer cells in the apoptotic response to mitotic arrest. The variability in clinical efficacy of taxane-based therapy is likely a reflection of this variability in apoptotic response, thus elucidation of the molecular mechanism of the apoptotic response to mitotic stress could lead to improved clinical strategies. To identify genes whose expression influences the rate and extent of apoptosis after mitotic arrest, we screened a kinase-enriched small interfering RNA library for effects on caspase activation in response to maximally effective doses of paclitaxel, a PLK1 inhibitor, or cisplatin. Small interfering RNA oligonucleotides directed against an atypical protein kinase, TP53RK, caused the greatest increase in caspase-3/7 activation in response to antimitotic agents. Time-lapse microscopy revealed that cells entered mitosis with normal kinetics, but died after entry into mitosis in the presence of paclitaxel more rapidly when TP53RK was depleted. Because expression levels of TP53RK vary in cancers, TP53RK levels could provide a molecular marker to predict response to antimitotic agents. TP53RK inhibition may also sensitize cancers to taxanes. *Cancer Res; 70(15); 6325–35. ©2010 AACR.*

Introduction

Paclitaxel, a broadly used cancer drug, binds and stabilizes microtubules, causing cells to arrest in mitosis due to the activation of the spindle assembly checkpoint. The response rate is ~30%, and most responsive patients eventually relapse, thus, generating interest in understanding mechanisms of resistance to taxanes. Resistance mechanisms include high expression of efflux pumps, mutations in β1 tubulin, and aberrant expression of βIII tubulin (1–3). However, it is unlikely that the large number of taxane nonresponders can be accounted for by mutations in tubulin or upregulation of drug transporters. Recent work suggests that the apoptotic response to mitotic arrest is the key driver of efficacy in preclinical models (4), and a study evaluating serial fine needle aspirates from breast cancer patients showed that apoptosis, not mitotic arrest, predicted response to paclitaxel (5). In addition to microtubule-binding agents, there are investigational drugs that inhibit mitotic kinesins or kinases (6, 7). Thus, understanding of the molecular mechanisms that determine apoptotic response to antimitotic agents will be critical to patient selection for taxanes as well as novel agents.

Authors' Affiliations: [1]Research Oncology, [2]Molecular Biology, and [3]Non-clinical Statistics, Genentech, Inc., South San Francisco, California

Note: Supplementary data for this article are available at Cancer Research Online (http://cancerres.aacrjournals.org/).

Corresponding Author: Lisa D. Belmont, Genentech, 1 DNA Way, 411A, South San Francisco, CA. Phone: 650-255-7523; Fax: 6502255770; E-mail: belmont.lisa@gene.com.

doi: 10.1158/0008-5472.CAN-10-0015

Studies have elucidated some steps in mitotic activation of apoptosis. Although the initiating events are not clear, mitotic arrest activates c-jun NH_2-terminal kinase, which activates Bim by phosphorylating T56 (8), disrupting the sequestration of Bim by the dynein light chain (9). Bim protein levels also increase during mitotic arrest (10). After release, Bim binds to the antiapoptotic proteins, Bcl-2 and Bcl_{XL}, releasing Bax and Bak and allowing them to oligomerize and form mitochondrial pores. Mitochondrial outer membrane permeabilization commits cells to death through apoptosis (11). Bcl-2 and Bcl_{XL} also undergo inhibitory phosphorylation during mitosis and mitotic arrest (12–16). All these proapoptotic events occur in mitosis, yet most cells complete mitosis, even after mitotic delay, without dying. Therefore, these proapoptotic signals must be restrained, and some antiapoptotic signaling during mitosis has been discovered. Caspase-9 and caspase-2 are phosphorylated and inhibited by CDK1, the mitotic cyclin-dependant kinase (17, 18), and DAP5 promotes cap-independent translation of CDK1 and Bcl-2 during mitosis (19).

To identify additional regulators of mitotic induction of apoptosis, we executed a small interfering RNA (siRNA) chemosensitization screen to identify genes whose expression modulates the apoptotic response to paclitaxel, a PLK inhibitor (20), or cisplatin. We included cisplatin to distinguish siRNAs that specifically enhanced mitotic death from those that were general chemosensitizers, and we included the PLK inhibitor to determine if the effects were specific to paclitaxel or mitotic arrest in general. Our screen differs from previous siRNA chemosensitization screens because we used concentrations of drug that maximally induce cell cycle arrest to identify gene products that influenced the extent of apoptotis

Published OnlineFirst July 20, 2010; DOI: 10.1158/0008-5472.CAN-10-0015

rather than mitotic arrest, as in the case of previous enhancer screens performed at submaximal doses (21–24). Because of differences in design of the screen, the hits were largely distinct from hits identified in previous paclitaxel sensitization screens.

The strongest hit, TP53RK, is an atypical protein kinase that was first identified in an interleukin-2–activated cytotoxic T-cell subtraction library and shown to bind and phosphorylate p53 on S15 in the presence of an activating cellular lysate (25). Later studies showed that purified TP53RK is activated by phopshorylation at S250 by Akt (26). Elevated TP53RK levels are associated with tumor grade in colorectal adenocarcinoma and, thus, may be an indicator of poor prognosis (27). We characterized the effects of depletion of TP53RK on the kinetics of mitotic fate.

Materials and Methods

Cell lines and reagents

MES-SA, MES-SA/MX2, A549, RPE, and HeLa cells were obtained from the American Type Culture Collection; p53-deleted and parental Hct116 cells were obtained from the Vogelstein laboratory (28); and HeLa-expressing GFP-H2b were obtained from Hongtao Yu (29). MES-SA and MES-SA/MX2 were obtained in 2010; HeLa GFP-H2b and Hct116 p53-matched lines were obtained in 2007; A549, RPE, and HeLa cells were obtained in 2006. Cell line stocks were frozen within three passages of receipt, and defrosted stocks were used within 15 passages after thawing. Inducible p53 small hairpin RNA (shRNA) RPE cells were constructed using the pHUSH tetracycline-inducible retrovirus gene transfer vector (30–32) with a previously described hairpin sequence for p53 (33). All constructs were verified by sequencing. Gene knockdown was verified by quantitative reverse transcription-PCR. paclitaxel (LKT Laboratories, Inc.), cisplatin (Sigma), and BI2536 were dissolved in DMSO or PBS. CelltiterGlo, CaspaseGlo 3/7 (Promega), RNAiMax (Invitrogen), and TP53RK antibody (Abnova) were used as per manufacturer's recommendations.

Screening conditions and plate-based assays

A siRNA library consisting of four siRNA duplexes per gene and designed to target all known kinases and several kinase-regulatory proteins (778 genes) was purchased from Dharmacon. Confirmation and titration assays were performed in duplicate. shRNA-inducible cells were treated 24 hours before transfection and maintained in doxycyclin (0.2 μg/mL). Cells were reverse transfected (20 nmol/L siRNA) for 24 hours followed by 48 hours of drug exposure. Final drug doses were 200 nmol/L paclitaxel, 200 nmol/L BI2536, or 50 μmol/L cisplatin. For caspase inhibition, ZVAD was added 1 hour before drug addition. A minimal z' of 0.5 or 0.4 for the CelltiterGlo or CaspaseGlo 3/7, respectively, was required. Dose-response was analyzed using 4 parameter logistic fit (GraphPad Prism).

Statistical methods

For each test siRNA oligo, two-factor ANOVA was applied to the natural logarithms of the CellTiterGlo (CTG) response and the ratio of CaspaseGlo (CG) to CTG response. The two factors were oligo IDs and treatments (e.g., paclitaxel versus DMSO). The estimates of the interaction terms between the two factors were extracted from the ANOVA analyses, along with the estimates were the SEMs, *P* values, and computed q-values. The interaction terms can be considered as the fold change between the changes of treatment effects (e.g., paclitaxel versus DMSO) of two oligonucletides. Oligonuceotides were first selected based on the computed q-values of <0.10, then a hit list was generated of genes for which two or more of its oligonucleotides had q-values of <0.10. If the effect is >0 (in log scale), then the effect was termed synergistic; if the effect was <0 (in log scale), then the effect was termed antagonistic.

Messenger RNA quantification

Messenger RNA was measured with Quantigene2.0 (Panomics) and normalized to cyclophilin. TP53RK Dharmacon siRNA were TP53RK-6 (D-003108-6), BCL2L1 (J-003458-14), and BUBR1 (L-004101-00).

Flow cytometry

hTERT-RPE P53(−) shRNA and HELA cells were transfected with siRNA for 24 hours then treated with 200 nmol/L paclitaxel. At varying times posttreatment, live cells were harvested and stained with propidium iodide (Fluka) or Annexin V FITC/propidium iodide (Millipore), and analyzed on FACSCaliber (Becton Dickinson), or cells were fixed overnight with 70% ethanol and stained with propidium iodide.

Time-lapse microscopy

GFP-H2B–expressing cells were plated on glass-bottomed 24-well plates (Greiner Bio-one) and transfected with indicated siRNA for 24 hours before addition of drug. Fluorescent and phase-contrast images were recorded with a ×10 objective every 15′ on an AxioObserver inverted microscope (Carl Zeiss) equipped with an environmental chamber (Okolab), an MS2000 XY stage (Applied Scientific Instruments, Inc.), and a CoolSnap CCD camera (HP). The chamber was maintained at 37°C, 5% CO_2. Devices were controlled using Slidebook (Intelligent Imaging Design).

Results

Identification and validation of screening conditions

We validated our screening procedure using TTK1 and BubR1 as antagonist controls (34), and BCL2L1 (which encodes Bcl_{XL} and Bcl_{XS}) as an agonist control (35). Depletion of TTK1 or BubR1 dampened the paclitaxel dose response as measured by cellular ATP using CellTiterGlo. BCL2L1 depletion causes a slight increase in the maximum inhibition (y_{min}) with CellTiterGlo, but does not provide an adequate signal for screening (Fig. 1A). To maximize signal, we measured the activation of caspase-3 and caspase-7 using a luminescence assay (CaspaseGlo3/7). The total caspase activation signal will be reduced under conditions in which cell cycle arrest precedes apoptosis due to the decreased cell number. To minimize contributions of cell cycle arrest, we normalized caspase activation to CellTiterGlo signal, which we used as a

Published OnlineFirst July 20, 2010; DOI: 10.1158/0008-5472.CAN-10-0015

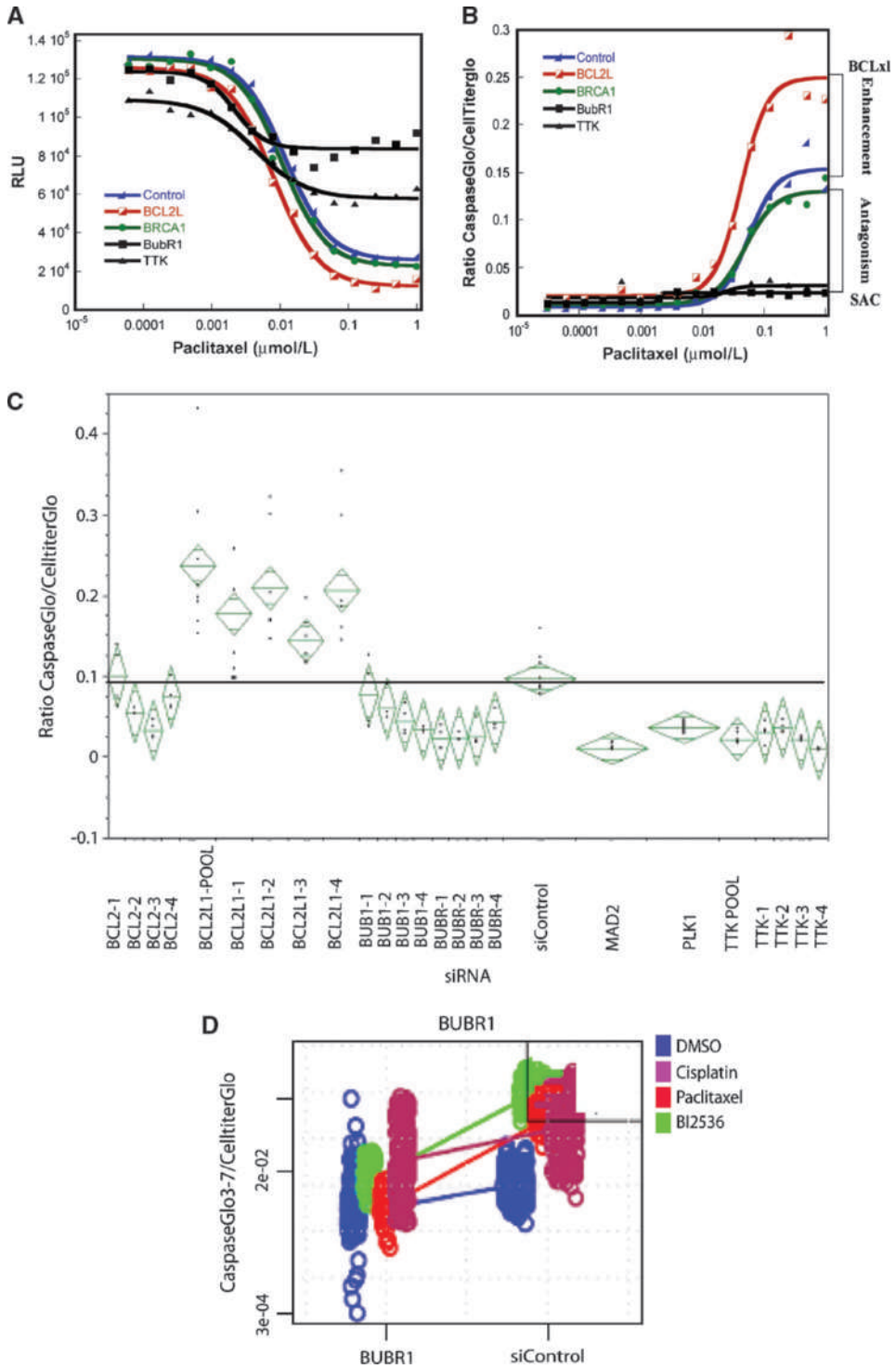

Figure 1. Identification and validation of screening conditions. A, cells were transfected with siRNA directed against the indicated genes and treated with paclitaxel. CellTiter was used to quantify ATP content after 48 h of drug exposure. B, caspase-3/7 activation normalized to total ATP for the same treatments shown in A. C, results of a test screen of known synergistic and antagonistic siRNAs treated with paclitaxel using the normalized caspase-3/7 activation assay. The top and bottom tips of the diamonds are 95% confidence intervals, and the line is the mean of replicates. Groups in which the diamonds do not overlap on the *Y* axis are considered to be significantly different. D, two-way ANOVA to evaluate the contributions of BubR1 depletion on response to indicated drugs.

Published OnlineFirst July 20, 2010; DOI: 10.1158/0008-5472.CAN-10-0015

surrogate for cell number. This gives a better estimate of caspase activation per cell (Fig. 1B).

In a 384-well plate format, three of four of the BCL2L1 siRNAs significantly increased apoptosis in response to paclitaxel, and all four siRNAs directed against BubR1 decreased apoptosis in response to paclitaxel (Fig. 1C). The *P* values for the four BubR1 siRNAs ranged from 2×10^{-30} to 7×10^{-20}. We concluded that these were suitable screening conditions, and screened hTERT immortalized RPE cells harboring an inducible shRNA directed against p53. With this cell line, we could start with a relatively normal genetic background and assess the contribution of p53 to maintenance of cell viability.

Identification of siRNAs that alter the response of cells to paclitaxel, cisplatin, and a PLK inhibitor

We screened a kinase-enriched library of synthetic siRNAs containing four siRNA oligonucleotides for each target. An example of the analysis (Fig. 1D) illustrates that BubR1 siRNA antagonizes the apoptotic response to paclitaxel or BI2536 (increased slope compared with DMSO control), but not cisplatin (slope parallel to that of the DMSO control). Using a false discovery rate of 10% (q value < 0.1), we identified all the significant interactions from 60,000 data points. These interactions included 115 siRNA targets that enhanced apoptotic response to paclitaxel, 198 siRNA targets that enhanced response to BI2536, and 58 that enhanced response to cisplatin. Examples of screening data are show for two hits, TP53RK and BRAF (Fig. 2A). TP53RK-6 (D-003108-06) enhanced the apoptotic response to paclitaxel and BI2536, whereas TP53RK-7 only enhanced the BI2536 response. Both siRNA oligos reduced levels of TP53RK, but TP53RK-6 was much more effective than TP53RK-7 (Fig. 3B), suggesting different thresholds for effect on paclitaxel versus BI2536 response. Two BRAF-directed siRNA oligonucleotides specifically reduced the apoptotic response to BI2536 (Fig. 2A).

Because a large number of hits were statistically significant, we set a threshold for biological significance. A 2-fold change in apoptotic response is consistently observed with siRNA directed against the positive controls for enhancement (BCL2L1) and antagonism (BubR1), so we selected genes for which at least two independent siRNA oligonucleotides caused a 2-fold or greater change in apoptotic response (Supplementary Table S1). We identified 52 genes whose depletion enhanced the apoptotic effects of paclitaxel by the above criteria. Of these, 21 were also identified as enhancers of BI2536, whereas only 9 overlapped with cisplatin hits. Only three hits were common to all three, suggesting that most were not general chemosensitizers. The antagonistic siRNA targets displayed even greater overlap between paclitaxel and BI2536. Of the 52 paclitaxel antagonists, 30 were identified in the BI2536 screen, whereas only 7 overlapped with cisplatin hits. siRNA targets that antagonized the apoptotic response to paclitaxel or BI2536 included many proteins required to maintain mitotic arrest, TTK, BubR1, Aurora B kinase, and CDK1. This is expected and increases our confidence that the hits identified in the screen are mechanism dependent. The hits from the paclitaxel sensitization screen were classified into functional classifications using Ingenuity software. After the more general categories such as amino acid metabolism and posttranslational modification (reflective of the kinase bias of the library), we noted a significant number of hits related to cell death and cell cycle. Cell death–related hits were more prevalent in the paclitaxel enhancer list, and cell cycle and cell proliferation hits were more prevalent in antagonist hits (Fig. 2B).

Confirmation of hits that enhance apoptotic response to paclitaxel

To evaluate the confirmation rate of the screen, we tested 20 of the top hits for enhancement of paclitaxel or BI2536 response with a 10-point dose response. Eight of 20 hits confirmed in this assay, giving a confirmation rate of 40% (Fig. 2C). There were no genes in the set of 20 tested that caused a significant shift in the CaspaseGlo/CelltiterGlo EC_{50} compared with the control siRNA. This is consistent with our assumption that potentiation of the paclitaxel response increases maximum caspase activation rather than shifting the EC_{50}. siRNA directed against TP53RK (also known as PRPK) gave the strongest increase in paclitaxel-induced apoptosis (Fig. 2C and D), so we focused on it for detailed analysis.

Of the four TP53RK-directed siRNA oligonucleotides, TP53RK-6 caused the greatest enhancement of caspase activity in response to BI2536, and TP53RK-7 caused a modest increase (Fig. 3A). Quantification of mRNA and Western blotting confirmed that TP53RK-6 was the most effective at depleting TP53RK (95% mRNA reduction), and TP53RK-7 had a more modest effect (~60% mRNA reduction; Fig. 3B and C). The other two siRNAs were not effective at reducing TP53RK levels and did not have a significant effect on the apoptotic response to antimitotic agents. Thus, extent of TP53RK depletion correlated with the biological effect of apoptotic enhancement.

TP53RK has p53-dependent and p53-independent effects on apoptosis

TP53RK has been reported to phosphorylate p53 on Ser15 (25). To determine if p53 was essential for TP53RK function, we used RPE cells that express a doxycycline-inducible shRNA directed against p53, and Hct116 cells with homozygous chromosomal deletions of p53 (28). We measured the effects of BCL2L1 or TP53RK depletion in the pairs of p53+/– cell lines. Depletion of BCL2L1 had similar effects on enhancement of caspase activity irrespective of p53 status, resulting in a 2- or 3-fold increase in caspase-3/7 activity in Hct116 and RPE cells, respectively. However, the effects of TP53RK depletion were greater in the cell lines with wild-type p53 compared with the p53 minus pair (Fig. 3D). Thus, depletion of TP53RK causes a p53-dependent and a p53-independent increase in paclitaxel-induced caspase activation.

TP53RK depletion increases the rate at which paclitaxel-treated cells die after entry into mitosis

We performed flow cytometry of RPE cells transfected with siRNA directed against TP53RK, PLK1, BCL2L1, or a control and exposed to paclitaxel. As expected, cells transfected with siRNA oligonucleotides directed against PLK1 accumulated with 4N DNA content. By 24 hours after paclitaxel treatment,

Published OnlineFirst July 20, 2010; DOI: 10.1158/0008-5472.CAN-10-0015

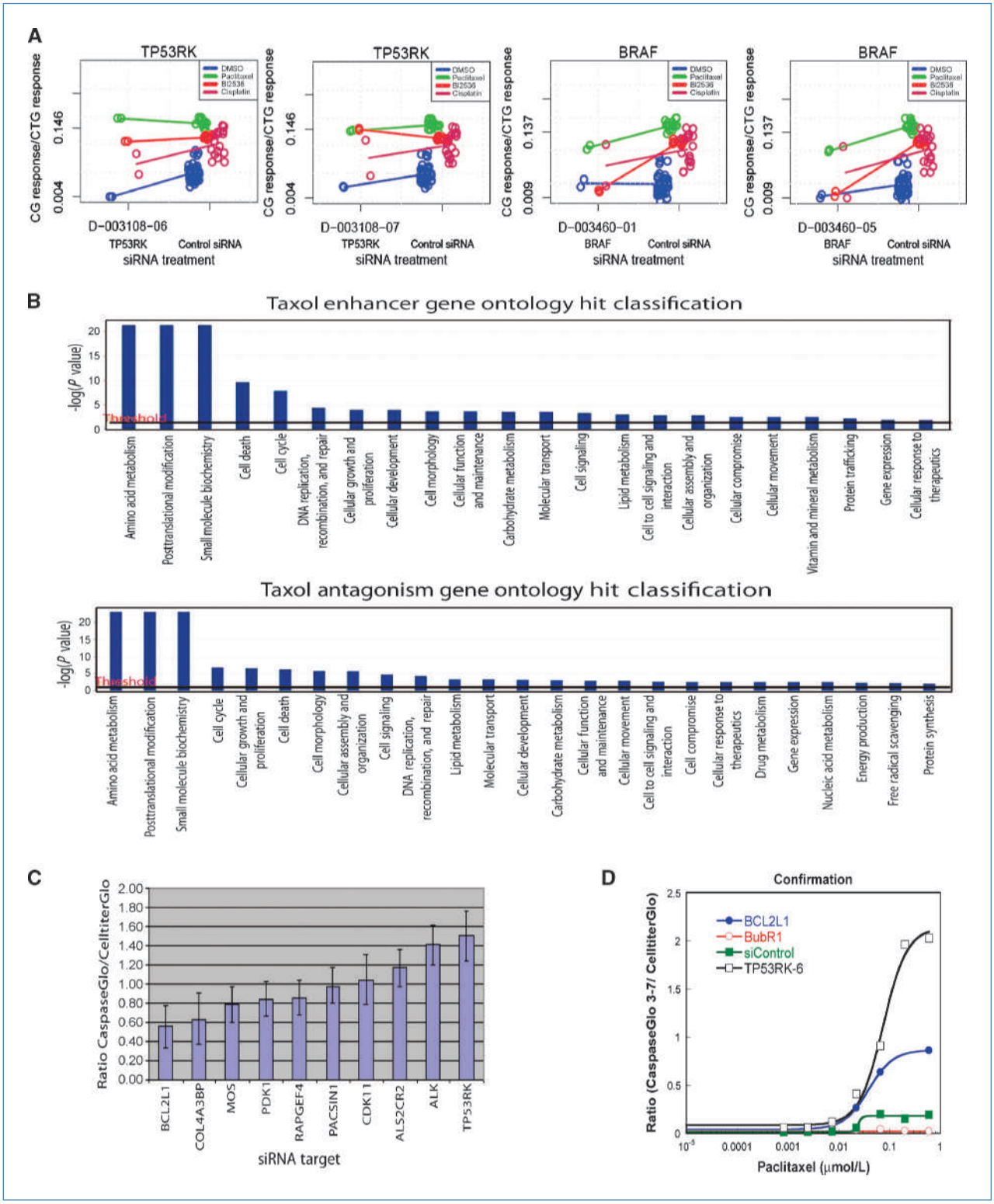

Figure 2. Hit confirmation. A, interaction plots of TP53RK- and BRAF-directed siRNA oligonucleotides. B, summary of hits from screen of RPE cells treated with paclitaxel. Paclitaxel enhancement and antagonist hits were classified using gene ontology molecular and cellular function category from Ingenuity software. The threshold line is a *P* value of 0.05. C, confirmed hits from the top 20 paclitaxel synergizers. CaspaseGlo/CelltiterGlo ratio at 600 nmol/L paclitaxel is shown. Hit confirmation required that at least two of four siRNA directed against a target have a *P* value of <0.01. Columns, mean; bars, SD. D, confirmation dose response for TP53RK siRNA and screening controls.

Published OnlineFirst July 20, 2010; DOI: 10.1158/0008-5472.CAN-10-0015

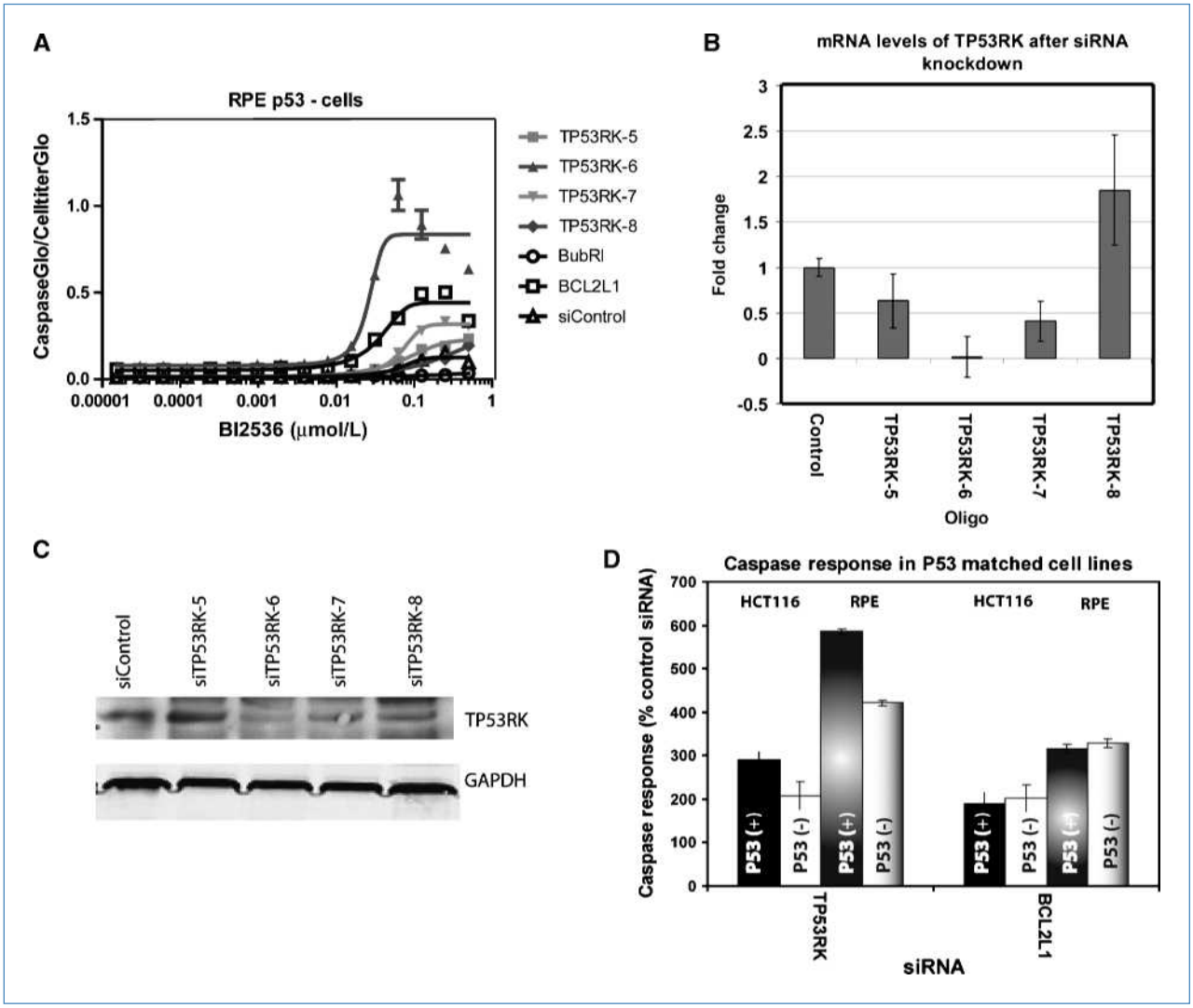

Figure 3. Extent of TP53RK depletion correlates with chemosensitization. A, CaspaseGlo 3/7 activation in response BI2536 after siRNA transfection with the indicated siRNA. B, mRNA levels of cells transfected with indicated siRNAs for TP53RK in RPE cells. C, Western blots of TP53RK in RPE cells transfected with TP53RK siRNA. The number represents the number of the siRNA oligonucleotides in A and B, and in Fig. 2A. siC is the control siRNA. D, paclitaxel induced caspase-3/7 activation in HCT116 p53 wt and null, and RPE p53 (+) and (–) cell lines transfected with siRNA directed against TP53RK or BCL2L1. Average of three experiments; columns, mean; bars, SD.

the control siRNA cells had accumulated with 4N DNA content; however, cells transfected with TP53RK, PLK1, or BCL2L1 oligonucleotides had already accumulated with sub2N DNA content. The siRNA control cells accumulated with sub2N DNA content by 48 hours posttreatment (Fig. 4A). To confirm increased apoptosis after paclitaxel in TP53RK or BCL2L1 depletion, we performed a time course using Annexin V and propidium idodide. The peak of Annexin V staining is observed 36 hours after paclitaxel addition, whereas the percent of cells that are permeable to propidium iodide plateaus later (Supplementary S1; Fig. 4B). To confirm that cells were dying due to apoptosis after mitotic entry, we performed Western blots on synchronized cells. SiRNA-transfected cells were released from S phase into paclitaxel and harvested before mitotic entry and during mitotic arrest. Cyclin B levels were monitored to confirm mitotic arrest. Caspase-3 cleavage was evident at an earlier time point after mitotic entry in BCL2L1- and TP53RK-depleted cells compared with control. It was difficult to detect caspase-3 in HeLa cells, so we evaluated poly ADP ribose polymerase (PARP), which is cleaved more completely after TP53RK and BCL2L1 depletion. In Hct116 cells, we also noted that levels of bim and noxa were higher at earlier time points during mitotic arrest in TP53RK or BCL2L1-depleted cells. To confirm that the observed effects were dependent on the cellular response to paclitaxel, we assayed cells that overexpress P-gp (MES-SA/MX2), resulting in a 100-fold diminished sensitivity to paclitaxel. The parent cells (MES-SA) were sensitized to paclitaxel after TP53RK depletion. The P-gp–expressing cells also exhibited increased cell death in response to paclitaxel after TP53RK depletion,

Published OnlineFirst July 20, 2010; DOI: 10.1158/0008-5472.CAN-10-0015

but required100-fold higher concentrations of paclitaxel. To confirm that sensitization was caspase dependent, we repeated the confirmation assay in the presence of the caspase inhibitor, ZVAD. This completely blocked response in control and TP53RK-depleted cells (Fig. 4D). Taken together, these data show that depletion of TP53RK accelerates the rate and extent of apoptosis after exposure to maximally effective doses of paclitaxel, and that the effect is dependent on caspase activity the response to pacitaxel.

For more detailed kinetic and morphologic analysis, we performed live cell time-lapse microscopy on Hct116 and HeLa cells expressing GFP-H2b (36, 37). The mitotic fates observed were completion of mitosis, mitotic slippage, or death before mitotic exit (Fig. 5A). We could clearly distinguish interphase and mitotic nuclei (Fig. 5B). We used the phase-contrast images to identify cell death, which we defined as the time at which the cells ceased blebbing, the plasma membrane was ruptured, and cytoplasm leaked of the cell. Most HeLa cells died before mitotic exit when exposed to 200 nmol/L paclitaxel, and depletion of TP53RK or BCL2L1 did not significantly change this. However, Hct116 cells exhibited a more variable fate, with 55% of the cells dying before mitotic exit and ~18% of the cells undergoing mitotic slippage. Depletion of BCL2L1 or TP53RK

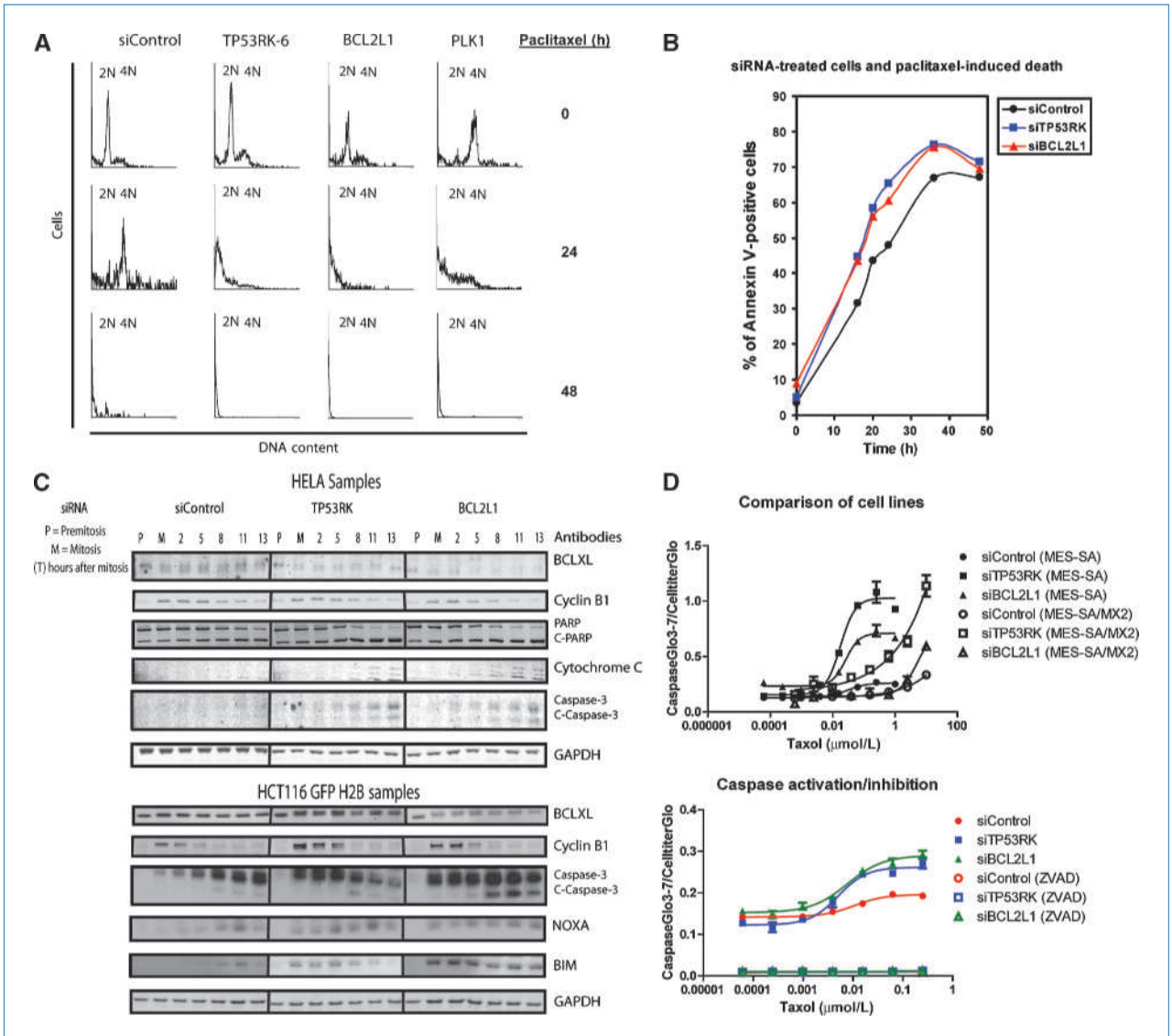

Figure 4. TP53RK depletion increases the rate of cell death after exposure to paclitaxel. A, histograms of DNA content of RPE cells transfected with siRNA for 24 h and then treated with 200 nmol/L paclitaxel for the indicated time. B, kinetic analysis of 200 nmol/L paclitaxel treatment showing Annexin V staining in siRNA-transfected HeLa cells. C, Western blot of apotosis/cell cycle–related proteins in synchronized HeLa and Hct116 H2b-GFP cells treated with 200 nmol/L paclitaxel after release from the second S-phase block. D, top, paclitaxel induced caspase-3/7 activation of siRNA-transfected MES-SA and MES-SA/MX2 cells. Bottom, paclitaxel induced caspase-3/7 activation of siRNA-transfected HELA cells treated with and without 10 μmol/L ZVAD.

Published OnlineFirst July 20, 2010; DOI: 10.1158/0008-5472.CAN-10-0015

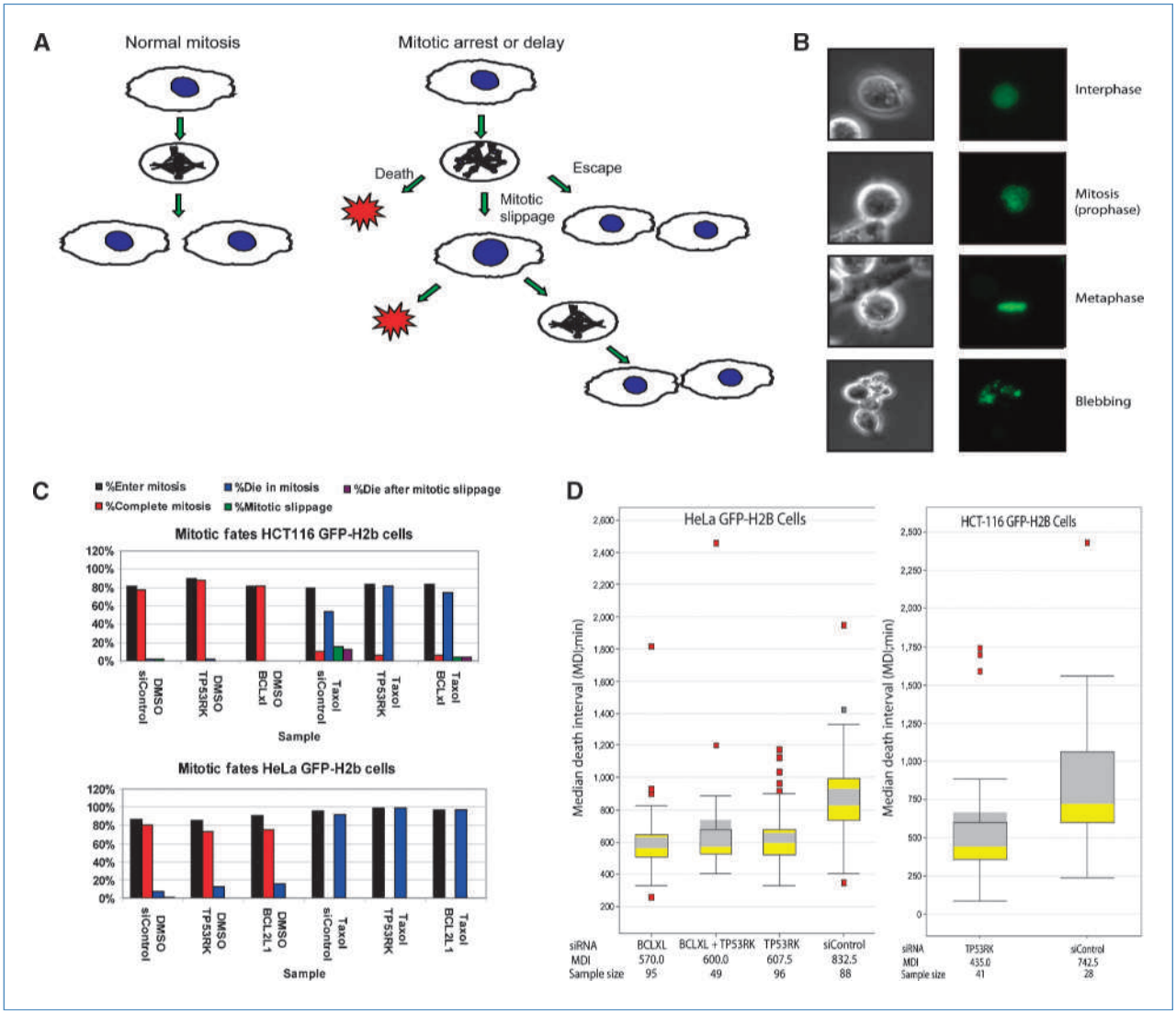

Figure 5. Time-lapse microscopy to evaluate kinetics of mitotic fate. A, cell fates after mitotic stress. B, example cell phase-contrast and fluorescent images of HeLa GFP-H2b cells in various stages of the cell cycle and apoptosis. C, mitotic fates of cells transfected with siRNAs and treated with paclitaxel or DMSO. D, box and whisker plots showing timing of death in mitosis of siRNA-transfected HeLa GFP-H2b and HCT116 GFP-H2b cells treated with 200 nmol/L paclitaxel. Yellow box, 25th to 75th percentile; gray boxes, the 95% confidence interval.

decreased the percentage of cells that underwent mitotic slippage and increased the percentage that died before mitotic exit (Fig. 5C). Dramatic effects were observed in kinetics of the apoptotic response to paclitaxel. Depletion of BCL2L1 did not affect duration of mitosis in nontreated cells, but significantly reduced the time between mitotic entry and cell death in the presence of paclitaxel in HeLa and Hct116 cells (Fig. 5D). We defined this as the mitotic death interval. The average mitotic death interval was decreased by ~4 hours in the BCL2L1- or TP53RK-depleted HeLa cells compared with control. These differences were highly significant with P values of 3.5×10^{-16} and 8.4×10^{-15} for BCL2L1 and TP53RK, respectively. A similar effect was observed in TP53RK-depleted Hct116 cells (Fig. 5D). The timing of mitotic death by live cell microscopy correlated well with cytochrome C release, PARP, and caspase-3 cleavage in the synchronized cell experiments, ~10 hours for HeLa cells depleted of TP53RK or BCL2L1. The kinetics of cell death are faster in Hct116 cells, with the average mitotic death interval at 7 hours, consistent with the appearance of cleaved caspase-3 (Fig. 4C). Simultaneously depletion of TP53RK and BCL2L1 (Supplementary Fig. S1) did not enhance the effect on mitotic death interval (Fig. 5D), suggesting that both proteins are acting in the same pathway. We conclude that TP53RK opposes intrinsic apoptosis signals that result from mitotic stress.

Discussion

We executed a siRNA drug sensitization screen using paclitaxel, BI2536, and cisplatin at concentrations that maximally

Published OnlineFirst July 20, 2010; DOI: 10.1158/0008-5472.CAN-10-0015

induce cell cycle arrest. The choice of screening conditions was based on the observation that clinically achievable levels of antimitotic agents cause robust mitotic arrest and that efficacy depends on the efficiency with which mitotic arrest leads to cancer cell death. To maximize this signal, we measured the ratio of caspase activation to total ATP to separate the effects of cell cycle arrest from apoptosis. In addition, we performed our screen in a relatively normal genetic background of hTERT-immortalized retinal pigment epithelial cells. Our screen identified a largely distinct set of hits compared with previous screens in transformed cell lines at subefficacious doses. MacKeigan and colleagues (21) ran a screen in HeLa cells to identify kinases that promoted resistance to chemotherapuetic agents, and identified CDK6, CDK8, SGK, mTOR, FER, JIK, PLK2, and PINK. Of these, we identified CDK6 as a cisplatin sensitizer, and both CDK6 and CDK8 as weak paclitaxel sensitizers. A genome-wide paclitaxel sensitization screen run on H1155 cells identified 87 high-confidence hits that had no overlap with our hits (22). Finally, Swanton and colleagues (38) ran siRNA sensitization screens on three cell lines with KRAS mutations. There were a few overlapping hits for paclitaxel sensitization, including ALK, ARK5, CARKL, and COL4A3BP. Overlapping antagonist hits include proteins required to maintain mitotic arrest such as TTK, AURKB, and BUB1B. Although we had significant overlap in antagonists, our screen identified many unique paclitaxel sensitizers, as well as sensitizers to PLK1 inhibition.

Two interesting confirmed hits from our screen are CDK11 and ALK. CDK11 is required for centrosome maturation (39), required for sister chromatid cohesion (40), and has recently been shown to be a RanGTP-dependent microtubule stabilization factor that regulates the rate of spindle assembly (41). Other kinases required for mitotic progression, such as PLK1 and Aurora A kinase (STK6), scored as antagonistic in the screen, most likely because the individual effects of depletion or paclitaxel cause maximal mitotic arrest but no additional effect on cell death. Because CDK11 depletion enhances the apoptotic response to antimitotic agents, it may have an additional role in protecting cells from apoptosis. ALK depletion also enhances the apoptotic response to BI2536 and paclitaxel. Oncogenic ALK translocations have been identified in lymphoma (42) and non–small cell lung carcinoma (43), and there are efforts to develop inhibitors of ALK (44). If normal levels of ALK protect cancer cells from the cytotoxic effects of antimitotic agents, ALK inhibitors could have broader utility as chemopotentiating agents.

Depletion of BRAF made cells less sensitive to a PLK inhibitor, leading us to postulate that activating mutations of BRAF could sensitize cells to PLK inhibition. Interestingly, in xenograft studies of response to a PLK1 inhibitor, two of the five sensitive models, Colo-205 and HT29, have the V600E-activating mutation in BRAF (45). Thus, PLK inhibitors may be useful in cancers that have a high frequency of BRAF mutation, such as melanoma or colorectal cancer. This is consistent with work showing that Ras mutant cancer cells are more sensitive to antimitotic agents, including BI2536 (46).

Depletion of TP53RK caused the greatest increase in the apoptotic response to antimitotic agents in confirmation assays. Recent work has shown that there is variability in the fate of cancer cells in response to mitotic arrest (47–49). Cells either die directly from mitotic arrest, complete mitosis after a delay, or slip out of mitotic arrest without completing mitosis and cytokinesis (mitotic slippage). The cells that undergo mitotic slippage either die in the next cell cycle, arrest their cell cycle, or continue to proliferate. Using time-lapse microscopy and single cell analysis, we showed that depletion of either BCL2L1 or TP53RK decreases the time from entry into mitosis in the presence of paclitaxel to cell death. Although it has been hypothesized that the levels of Bcl-2 family members could influence the fate and kinetics of the apoptotic response to mitotic arrest (49), this is the first direct demonstration that manipulation of Bcl_X levels decreases the time from mitotic entry to cell death in the presence of an antimitotic agent. This is important to consider in the context of Bcl-2 and Bcl_{XL} inhibitors that are currently in clinical trials (11). Combining these Bcl-2 family antagonists with taxane-based chemotherapy could increase their efficacy in cancer cell killing during the window of time when the drug is present in the tumor at pharmacologically active concentrations.

siRNA depletion of TP53RK had a nearly identical effect of decreasing the time from mitotic entry to death. This was not

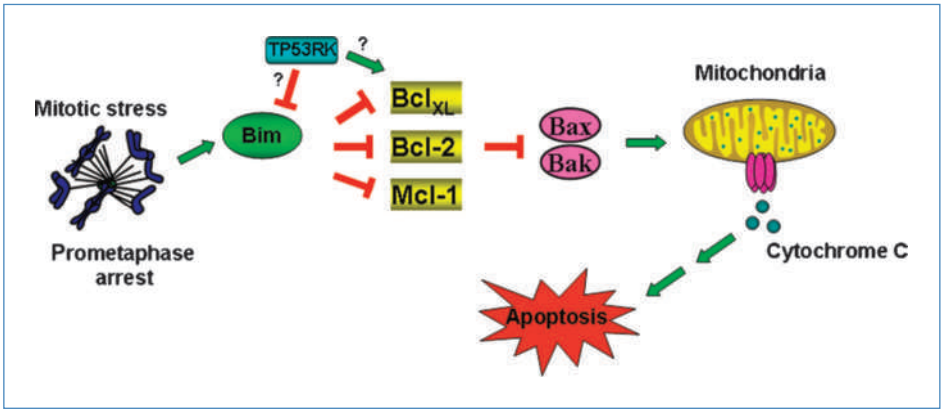

Figure 6. Proposed models of TP53RK regulating response to mitotic stress. TP53RK could act by inhibiting the activity of bim, either by promoting degradation or inhibiting its interaction with Bcl_{XL}. Alternatively, it could activate Bcl_{XL}.

Published OnlineFirst July 20, 2010; DOI: 10.1158/0008-5472.CAN-10-0015

expected from what is known about this protein. TP53RK was reported to phosphorylate p53 on Ser15, activating its proapoptotic activity (25, 50). We therefore might expect more survival upon depletion of TP53RK. However, p53 is also phosphorylated by ATR and ATM on Ser15 (51), making this activity redundant. p53 remains phosphorylated on Ser15 even after depletion of TP53RK,[4] suggesting that this is not the major role of TP53RK in proliferating cells.

Depletion of TP53RK and BCL2L1 had similar effects on the timing of cell during mitotic arrest, and simultaneous depletion of both TP53RK and BCL2L1 did not enhance the effect. This suggests that these proteins are acting within the same pathway. Because Bcl_{XL} sequesters Bax and Bak, we think it is unlikely that TP53RK acts downstream of Bcl_{XL}. We therefore propose two models by which TP53RK could regulate Bcl_{XL} during mitotic arrest. The first hypothesis is that TP53RK activates BCL_{XL} during mitotic arrest, and thus, its depletion effect is similar to that of BCL2L1 depletion. The second model is that TP53RK inhibits the activity of Bim, the BH3-only sensor protein that antagonizes the antiapoptotic effects of Bcl_{XL} and Mcl-1 in mitosis. TP53RK could act by decreasing the binding of Bim to Bcl_{XL} or by destabilizing Bim. It has been reported that Bim is phosphorylated by extracellular signal-regulated kinase, which primes it for phosphorylation by RSK1/2, leading to ubiquitin-mediated proteolysis (52). Distinct kinases could regulate Bim stability in mitosis, and TP53RK could have a role either in priming or directly phosphorylating the degron (Fig. 6).

The levels of TP53PK are variably expressed in cancer cells, suggesting that it might be useful as a predictive biomarker of response to antimitotic agents. In a study of breast cancer tissue, TP53RK was significantly overexpressed in lobular breast cancer versus normal tissue ($P = 1 \times 10^{-11}$) and in invasive ductal carcinoma versus normal ($P = 1.8 \times 10^{-12}$). In an independent breast cancer study, TP53RK was overexpressed in ductal breast carcinoma ($P = 1 \times 10^{-3}$; Oncomine). Our studies suggest that expression level of TP53RK may predict response to antimitotic agents such as taxanes, and inhibitors of mitotic kinases such as PLK1. Additionally, TP53RK may have potential as a drug target whose inhibition could sensitize cancer cells to taxanes or other antimitotic agents.

Disclosure of Potential Conflicts of Interest

No potential conflicts of interest were disclosed.

Acknowledgments

We thank Laura Corson and Thomas Hunsaker for the RPE cells expressing inducible p53 shRNA, and Hongtao Yu for the GFP-H2b–expressing HeLa cells.

The costs of publication of this article were defrayed in part by the payment of page charges. This article must therefore be hereby marked *advertisement* in accordance with 18 U.S.C. Section 1734 solely to indicate this fact.

Received 01/04/2010; revised 05/12/2010; accepted 06/08/2010; published OnlineFirst 07/20/2010.

[4] D. Peterson, unpublished.

References

1. McGrogan BT, Gilmartin B, Carney DN, McCann A. Taxanes, microtubules and chemoresistant breast cancer. Biochim Biophys Acta 2008;1785:96–132.
2. Kavallaris M. Microtubules and resistance to tubulin-binding agents. Nat Rev Cancer 2010;10:194–204.
3. Yin S, Bhattacharya R, Cabral F. Human mutations that confer paclitaxel resistance. Mol Cancer Ther 2010;9:327–35.
4. Milross CG, Mason KA, Hunter NR, Chung WK, Peters LJ, Milas L. Relationship of mitotic arrest and apoptosis to antitumor effect of paclitaxel. J Natl Cancer Inst 1996;88:1308–14.
5. Symmans WF, Volm MD, Shapiro RL, et al. Paclitaxel-induced apoptosis and mitotic arrest assessed by serial fine-needle aspiration: implications for early prediction of breast cancer response to neoadjuvant treatment. Clin Cancer Res 2000;6:4610–7.
6. Jackson JR, Patrick DR, Dar MM, Huang PS. Targeted anti-mitotic therapies: Can we improve on tubulin agents? Nat Rev Cancer 2007;7:107–17.
7. Bergnes G, Brejc K, Belmont L. Mitotic kinesins: prospects for antimitotic drug discovery. Curr Top Med Chem 2005;5:127–45.
8. Lei K, Davis RJ. JNK phosphorylation of Bim-related members of the Bcl2 family induces Bax-dependent apoptosis. Proc Natl Acad Sci U S A 2003;100:2432–7.
9. Puthalakath H, Huang DC, O'Reilly LA, King SM, Strasser A. The proapoptotic activity of the Bcl-2 family member Bim is regulated by interaction with the dynein motor complex. Mol Cell 1999;3:287–96.
10. Tan TT, Degenhardt K, Nelson DA, et al. Key roles of BIM-driven apoptosis in epithelial tumors and rational chemotherapy. Cancer Cell 2005;7:227–38.
11. Adams JM, Cory S. The Bcl-2 apoptotic switch in cancer development and therapy. Oncogene 2007;26:1324–37.
12. Scatena CD, Stewart ZA, Mays D, et al. Mitotic phosphorylation of Bcl-2 during normal cell cycle progression and Taxol-induced growth arrest. J Biol Chem 1998;273:30777–84.
13. Poruchynsky MS, Wang EE, Rudin CM, Blagosklonny MV, Fojo T. Bcl-xL is phosphorylated in malignant cells following microtubule disruption. Cancer Res 1998;58:3331–8.
14. Terrano DT, Upreti M, Chambers TC. Cyclin-dependent kinase 1-mediated Bcl-xL/Bcl-2 phosphorylation acts as a functional link coupling mitotic arrest and apoptosis. Mol Cell Biol 2010;30:640–56.
15. Yamamoto K, Ichijo H, Korsmeyer SJ. BCL-2 is phosphorylated and inactivated by an ASK1/Jun N-terminal protein kinase pathway normally activated at G(2)/M. Mol Cell Biol 1999;19:8469–78.
16. Upreti M, Galitovskaya EN, Chu R, et al. Identification of the major phosphorylation site in Bcl-xL induced by microtubule inhibitors and analysis of its functional significance. J Biol Chem 2008;283:35517–25.
17. Allan LA, Clarke PR. Phosphorylation of caspase-9 by CDK1/cyclin B1 protects mitotic cells against apoptosis. Mol Cell 2007;26:301–10.
18. Andersen JL, Johnson CE, Freel CD, et al. Restraint of apoptosis during mitosis through interdomain phosphorylation of caspase-2. EMBO J 2009;28:3216–27.
19. Marash L, Liberman N, Henis-Korenblit S, et al. DAP5 promotes cap-independent translation of Bcl-2 and CDK1 to facilitate cell survival during mitosis. Mol Cell 2008;30:447–59.
20. Steegmaier M, Hoffmann M, Baum A, et al. BI 2536, a potent and selective inhibitor of polo-like kinase 1, inhibits tumor growth *in vivo*. Curr Biol 2007;17:316–22.
21. MacKeigan JP, Murphy LO, Blenis J. Sensitized RNAi screen of

Published OnlineFirst July 20, 2010; DOI: 10.1158/0008-5472.CAN-10-0015

human kinases and phosphatases identifies new regulators of apoptosis and chemoresistance. Nat Cell Biol 2005;7:591–600.
22. Whitehurst AW, Bodemann BO, Cardenas J, et al. Synthetic lethal screen identification of chemosensitizer loci in cancer cells. Nature 2007;446:815–9.
23. Bartz SR, Zhang Z, Burchard J, et al. Small interfering RNA screens reveal enhanced cisplatin cytotoxicity in tumor cells having both BRCA network and TP53 disruptions. Mol Cell Biol 2006;26:9377–86.
24. Tsui M, Xie T, Orth JD, et al. An intermittent live cell imaging screen for siRNA enhancers and suppressors of a kinesin-5 inhibitor. PLoS One 2009;4:e7339.
25. Abe Y, Matsumoto S, Wei S, et al. Cloning and characterization of a p53-related protein kinase expressed in interleukin-2-activated cytotoxic T-cells, epithelial tumor cell lines, and the testes. J Biol Chem 2001;276:44003–11.
26. Facchin S, Ruzzene M, Peggion C, et al. Phosphorylation and activation of the atypical kinase p53-related protein kinase (PRPK) by Akt/PKB. Cell Mol Life Sci 2007;64:2680–9.
27. Capra M, Nuciforo PG, Confalonieri S, et al. Frequent alterations in the expression of serine/threonine kinases in human cancers. Cancer Res 2006;66:8147–54.
28. Bunz F, Dutriaux A, Lengauer C, et al. Requirement for p53 and p21 to sustain G_2 arrest after DNA damage. Science 1998;282:1497–501.
29. Tang Z, Sun Y, Harley SE, Zou H, Yu H. Human Bub1 protects centromeric sister-chromatid cohesion through Shugoshin during mitosis. Proc Natl Acad Sci U S A 2004;101:18012–7.
30. Gray D, Jubb AM, Hogue D, et al. Maternal embryonic leucine zipper kinase/murine protein serine-threonine kinase 38 is a promising therapeutic target for multiple cancers. Cancer Res 2005;65:9751–61.
31. Gray DC, Hoeflich KP, Peng L, et al. pHUSH: a single vector system for conditional gene expression. BMC Biotechnol 2007;7:61.
32. Hoeflich KP, Gray DC, Eby MT, et al. Oncogenic BRAF is required for tumor growth and maintenance in melanoma models. Cancer Res 2006;66:999–1006.
33. Brummelkamp TR, Bernards R, Agami R. A system for stable expression of short interfering RNAs in mammalian cells. Science 2002;296:550–3.
34. Sudo T, Nitta M, Saya H, Ueno NT. Dependence of paclitaxel sensitivity on a functional spindle assembly checkpoint. Cancer Res 2004;64:2502–8.
35. Vijapurkar U, Wang W, Herbst R. Potentiation of kinesin spindle protein inhibitor-induced cell death by modulation of mitochondrial and death receptor apoptotic pathways. Cancer Res 2007;67:237–45.
36. Kanda T, Sullivan KF, Wahl GM. Histone-GFP fusion protein enables sensitive analysis of chromosome dynamics in living mammalian cells. Curr Biol 1998;8:377–85.
37. Ban KH, Torres JZ, Miller JJ, et al. The END network couples spindle pole assembly to inhibition of the anaphase-promoting complex/cyclosome in early mitosis. Dev Cell 2007;13:29–42.
38. Swanton C, Marani M, Pardo O, et al. Regulators of mitotic arrest and ceramide metabolism are determinants of sensitivity to paclitaxel and other chemotherapeutic drugs. Cancer Cell 2007;11:498–512.
39. Petretti C, Savoian M, Montembault E, Glover DM, Prigent C, Giet R. The PITSLRE/CDK11p58 protein kinase promotes centrosome maturation and bipolar spindle formation. EMBO Rep 2006;7:418–24.
40. Hu D, Valentine M, Kidd VJ, Lahti JM. CDK11(p58) is required for the maintenance of sister chromatid cohesion. J Cell Sci 2007;120:2424–34.
41. Yokoyama H, Gruss OJ, Rybina S, et al. Cdk11 is a RanGTP-dependent microtubule stabilization factor that regulates spindle assembly rate. J Cell Biol 2008;180:867–75.
42. Morris SW, Kirstein MN, Valentine MB, et al. Fusion of a kinase gene, ALK, to a nucleolar protein gene, NPM, in non-Hodgkin's lymphoma. Science 1994;263:1281–4.
43. Soda M, Choi YL, Enomoto M, et al. Identification of the transforming EML4-ALK fusion gene in non-small-cell lung cancer. Nature 2007;448:561–6.
44. Li R, Morris SW. Development of anaplastic lymphoma kinase (ALK) small-molecule inhibitors for cancer therapy. Med Res Rev 2008;28:372–412.
45. Sutton D, Diamond M, Faucette M, et al. Efficacy of GSK461364, a selective Plk1 inhibitor, in human tumor xenograft models. AACR Meeting Abstracts 2007;2007:538.
46. Luo J, Emanuele MJ, Li D, et al. A genome-wide RNAi screen identifies multiple synthetic lethal interactions with the Ras oncogene. Cell 2009;137:835–48.
47. Shi J, Orth JD, Mitchison T. Cell type variation in responses to antimitotic drugs that target microtubules and kinesin-5. Cancer Res 2008;68:3269–76.
48. Gascoigne KE, Taylor SS. Cancer cells display profound intra- and interline variation following prolonged exposure to antimitotic drugs. Cancer Cell 2008;14:111–22.
49. Orth JD, Tang Y, Shi J, et al. Quantitative live imaging of cancer and normal cells treated with Kinesin-5 inhibitors indicates significant differences in phenotypic responses and cell fate. Mol Cancer Ther 2008;7:3480–9.
50. Dumaz N, Meek DW. Serine15 phosphorylation stimulates p53 transactivation but does not directly influence interaction with HDM2. EMBO J 1999;18:7002–10.
51. Nakagawa K, Taya Y, Tamai K, Yamaizumi M. Requirement of ATM in phosphorylation of the human p53 protein at serine 15 following DNA double-strand breaks. Mol Cell Biol 1999;19:2828–34.
52. Dehan E, Bassermann F, Guardavaccaro D, et al. βTrCP- and Rsk1/2-mediated degradation of BimEL inhibits apoptosis. Mol Cell 2009;33:109–16.

Published OnlineFirst July 20, 2010; DOI: 10.1158/0008-5472.CAN-10-0015

Cancer Research
The Journal of Cancer Research (1916–1930) | The American Journal of Cancer (1931–1940)

AACR American Association for Cancer Research

A Chemosensitization Screen Identifies TP53RK, a Kinase that Restrains Apoptosis after Mitotic Stress

David Peterson, James Lee, Xingye C. Lei, et al.

Cancer Res Published OnlineFirst July 20, 2010.